Available online at www.sciencedirect.com
ScienceDirect
Journal of Magnetic Resonance 183 (2006) 32–40
JMR Journal of Magnetic Resonance
www.elsevier.com/locate/jmr

High flow-resolution for mobility estimation in 2D-ENMR of proteins using maximum entropy method (MEM-ENMR) ☆

Sunitha B. Thakur, Qiuhong He *,[1]

Departments of Medical Physics and Radiology, Memorial Sloan-Kettering Cancer Center, New York, NY 10021, USA

Received 2 May 2006; revised 8 July 2006
Available online 9 August 2006

Abstract

Multidimensional electrophoretic NMR (nD-ENMR) is a potentially powerful tool for structural characterization of co-existing proteins and protein conformations. By applying a DC electric field pulse, the electrophoretic migration rates of different proteins were detected experimentally in a new dimension of electrophoretic flow. The electrophoretic mobilities were employed to differentiate protein signals. In U-shaped ENMR sample chambers, individual protein components in a solution mixture followed a cosinusoidal electrophoretic interferogram as a function of its unique electrophoretic migration rate. After Fourier transformation in the electrophoretic flow dimension, the protein signals were resolved at different resonant frequencies proportional to their electrophoretic mobilities. Currently, the mobility resolution of the proteins in the electrophoretic flow dimension is limited by severe truncations of the electrophoretic interferograms due to the finite electric field strength available before the onset of heat-induced convection. In this article, we present a successful signal processing method, the Burg's maximum entropy method (MEM), to analyze the truncated ENMR signals (MEM-ENMR). Significant enhancement in flow resolution was demonstrated using two-dimensional ENMR of two protein samples: a lysozyme solution and a solution mixture of bovine serum albumin (BSA) and ubiquitin. The electrophoretic mobilities of lysozyme, BSA and ubiquitin were measured from the MEM analysis as 7.5×10^{-5}, 1.9×10^{-4} and 8.7×10^{-5} $cm^2\ V^{-1}\ s^{-1}$, respectively. Results from computer simulations confirmed a complete removal of truncation artifacts in the MEM-ENMR spectra with 3- to 6-fold resolution enhancement.

Keywords: Electrophoretic NMR (ENMR); NMR signal separation of co-existing proteins; Heat-induced convection in ENMR; Burg's maximum entropy method (MEM); Flow-resolution enhancement

1. Introduction

NMR methods are well-developed for characterizing structures of pure proteins, strongly bound protein-protein or protein-ligand complexes [1,2]. The current NMR methods, however, have difficulties in resolving overlapping NMR signals from co-existing protein components for structural analysis in the presence of weak protein interactions. Such characterization of multiple proteins and nucleic acids *in situ* has the potential of providing fundamental understanding of biological signaling processes. We have previously developed multi-dimensional electrophoretic NMR (ENMR) techniques to resolve overlapping NMR resonances of mixed proteins in solution [3]. The idea of electrophoretic NMR was first demonstrated in the so-called "DC NMR" experiment on a low-resolution electromagnetic NMR spectrometer by Holz et al. [4–6]. Following this "concept-proven" experiment, Saarinen and Johnson [7] successfully carried out a high-resolution ENMR experiment to measure the electrophoretic mobilities of different ionic species in a free mixture solution.

☆ Some of the preliminary results were reported in the 43rd Experimental Nuclear Magnetic Resonance Conference (ENC), Savannah, Georgia, March 30–April 4, 2003.

* Corresponding author. Fax: +1 412 647 9800.
E-mail address: heq@upmc.edu (Q. He).
[1] Present address: Departments of Radiology and Bioengineering/University of Pittsburgh Cancer Institute, Magnetic Resonance Research Center, B-804 PUH-UPMC, University of Pittsburgh, 200 Lothrop Street, Pittsburgh, PA 15213, USA.

1090-7807/$ - see front matter © 2006 Elsevier Inc. All rights reserved.
doi:10.1016/j.jmr.2006.07.009

Subsequently, He and Johnson developed the two-dimensional spin-echo ENMR (SE-ENMR) [8] and stimulated echo ENMR (STE-ENMR) spectroscopy [9,10] to introduce a new dimension of electrophoretic flow to the corresponding one-dimensional NMR spectrum. Since the NMR resonant frequencies in the new flow dimension are determined by the electrophoretic mobilities of the migrating molecules, it is therefore possible to separate overlapping signals of different ionic species mixed in solution in the flow dimension [9,11–14]. Directions of electrophoretic migration were determined using cylindrical sample chambers and linear prediction method for signal reconstruction [13,14]. Expansion of the 2D-ENMR to more dimensions has been demonstrated by a successful experiment of three-dimensional electrophoretic correlation NMR spectroscopy (3D EP-COSY) [15]. As demonstrated in the three-dimensional EP-COSY experiment, individual 2D NMR spectra of several molecules may be obtained from a mixture solution in order to achieve simultaneous protein structural determination [3]. In these ENMR experiments, an additional dimension of electrophoretic flow was introduced to a 1D or 2D NMR spectra by applying a DC electric field. The NMR signals in the flow dimension can be modeled using classical Bloch equations, independent of internal spin dynamics of the protein components. When using U-shaped ENMR sample tubes, a cosinusoidal modulated ENMR signal in the flow dimension is a product of net magnetization from a conventional NMR experiment and a cosine factor. This is a function of the amplitude and duration of applied DC electric pulse and electrical conductivity of the sample solution. The ENMR signal modulation is also determined by the amount of electric current passing through the ENMR sample chamber of cross-sectional area A.

For proteins in biological buffer solutions of high-ionic conductivity (κ), the available electric current is limited due to heat-induced convection. In ENMR experiments employing sample chambers of large cross-sectional area, severe heat-induced convection prevents ENMR measurements in sample solutions of high-ionic strength. To address this issue, He and co-workers have developed the capillary array ENMR (CA-ENMR) method [16] and convection-compensated ENMR techniques (CC-ENMR) [17]. In CA-ENMR, physical barriers were imposed using bundled capillaries to restrict the heat-induced convection current. In the CC-ENMR, the convective phase distortions in an ENMR spectrum were removed by employing the gradient moment nulling techniques, as well as by switching the polarity of DC electric field. In these ENMR experiments, however, the ENMR interferograms were severely truncated, leading to spectroscopic artifacts that limited signal resolution in the flow dimension. More suitable signal processing algorithms are needed to alleviate the truncation artifacts in the analysis of multidimensional ENMR data. Here, we report the results of an ENMR analysis using Burg's maximum entropy method (MEM) [18,20–23]. MEM has had successful applications in the spectral analysis of high-resolution NMR [24–28] and NQR data [29]. In our method, removal of truncation artifacts enhanced the ENMR spectral resolution in the flow dimension, facilitating accurate measurements of electrophoretic mobilities of protein components in mixed protein solutions.

2. Theory

2.1. Electrophoretic NMR

The stimulated echo ENMR (STE-ENMR) pulse sequence, $90^\circ - \tau[\delta,g] - 90^\circ - \Delta(E_{dc};\delta_c,g_c) - 90^\circ - \tau[\delta,g] - acq$, [9,10] was used to demonstrate the effectiveness of the MEM algorithms in ENMR spectral analysis. In STE-ENMR, the electrophoretic migration of molecules in the U-tube modulated the stimulated echo signal by a cosine factor, $\cos(KE_{dc}\Delta\mu)$ [9],

$$M(E_{dc}) = \frac{M_0}{2}\exp\left[-D_{\mathrm{m}}K^2\left(\tau_{\mathrm{D}} - \frac{\delta}{3}\right) - \frac{2\tau}{T_2} - \frac{\Delta}{T_1}\right] \times \cos((KE_{dc}\Delta)\mu) \quad (1)$$

The cosinusoidal modulation frequency $KE_{dc}\mu$ is proportional to the electrophoretic mobility μ. The parameter $K = \gamma g\delta$ characterizes the magnetization helix pitch by the pulsed field gradients of amplitude g and duration δ, and the gyromagnetic ratio of the nucleus, γ [9]. The exponential term collects the contributions from the spin–spin T_2 relaxation decay during delay τ, the spin–lattice T_1 relaxation effect during delay Δ, and the molecular diffusion (D_{m}) during the delay $\tau_{\mathrm{D}} = 2\tau + 2p_{\mathrm{w}} + \Delta$, where p_{w} is the duration of the 90° pulse. A crusher gradient of the amplitude and duration of g_c and δ_c was applied during T_1 spin storage time. The electric field was applied between the last two 90° pulses along the direction of the magnetic field gradients, parallel to the B_0 direction.

In multidimensional ENMR of molecular mixtures, Fourier transformation of the electrophoretic interferogram (Eq. (1)) versus E_{dc} exhibits a pair of symmetrical ENMR resonances characterized for each migrating molecule 'i' in the flow dimension as

$$\upsilon_i = \pm[(K\Delta\mu_i)/(2\pi\kappa A)], \quad (2)$$

where υ_i is the elecrophoretic frequency and is proportional to μ_i, the mobility of the molecular component 'i'. The spectral resolution in the electrophoretic flow dimension is defined as [9],

$$R_{\mathrm{ENMR}} = \upsilon_i/\delta\upsilon_i, \quad (3)$$

where $\delta\upsilon_i$ is the full width at half height (FWHH) of the peak from the ith component. In fast Fourier transform (FFT) analysis of the truncated electrophoretic interferograms, $\delta\upsilon_i$ is dominated by the sinc point spread function with reduced spectral resolution. In MEM, $\delta\upsilon_i$ nearly gives a Dirac delta function as point spread function, resulting in

improved spectral resolution in flow dimension as compared to FFT.

2.2. Maximum entropy method (MEM)

The basic idea of Burg's maximum entropy method for spectral analysis [18,20–23] relies on an estimate of the power spectrum of a truncated input data series (y_n, $n = 1,\ldots,N$) in the time domain,

$$y_N = a_1 y_{N-1} + a_2 y_{N-2} + \ldots.. + a_k y_{N-k} + W_N, \tag{4}$$

where W_N is Gaussian white noise, and $a_1,\ldots,a_k$ are coefficients determining the power spectrum of the time series data. The signals y_k are first conditioned to have a mean of zero by subtracting the sample mean $\bar{y} = \frac{1}{N}\sum_{k=1}^{N} y_k$ from the original signal y_k, and are then fitted to an auto regression (AR) model (Eq. (4)).

The power spectral density $P(\omega)$ at a frequency 'ω' of the discrete time series in Eq. (4) is related to the auto-correlation coefficients $r(k)$,

$$P(\omega) = \sum_{k=-N}^{N} r(k) e^{ik\omega}, \tag{5}$$

where $r(-k) = r(k)^*$ represents the complex conjugate, and

$$r(k = -m,\ldots m) = \sum_{j=0}^{N-k} y_j^* y_{k+j} \tag{6}$$

is the autocorrelation function of a time series $\{y_i\}$ and $m \leq N-1$. Although a unique solution of $P(\omega)$ cannot be found for finite time series, there may be multiple solutions, or spectra, that are consistent with the input data.

$$P(\omega) = \sum_{k=-m}^{m} r(k) e^{ik\omega} + \sum_{|k|>m} r(k) e^{ik\omega}, \tag{7}$$

$r(k)$, $|k| > m$ must be chosen so that $P(\omega) \geqslant 0$. Here, the principle of maximum entropy can be applied in order to obtain the optimal solution. Given autocorrelation $r(k), -m < k < m$, $r(k), |k| > m$ can be extrapolated to yield the power spectrum with maximum entropy, and hence the optimized model parameter. This is contingent on minimizing the sum of the forward and backward squared prediction errors, with the filter coefficients constrained to satisfy the Levinson–Durbin recursion [22,23]. The measured minimum uncertainty, or error between the real data and the modeled signals, is equivalent to the maximum Shannon entropy S as

$$S = \int \log P(\omega) d\omega. \tag{8}$$

MEM spectrum solution is given as

$$P_{\mathrm{mem}}(\omega) = \frac{E_m}{\left|1 + \sum_{k=1}^{m} a_k e^{ik\omega}\right|^2}, \tag{9}$$

where E_m is the prediction error of the filter. Since $r(k)$is given from $|k| \leqslant m$, the coefficients a_k can be found by solving the following equations:

$$\begin{bmatrix} r(0) & r^*(1) & \ldots\ldots & r_x^*(m) \\ r(1) & r(0) & \ldots\ldots & r^*(m-1) \\ \ldots\ldots & \ldots\ldots & \ldots\ldots & \ldots\ldots \\ r(m) & r(m-1) & \ldots\ldots & r(0) \end{bmatrix} \begin{bmatrix} 1 \\ a_1 \\ \ldots \\ a_m \end{bmatrix} = E_m \begin{bmatrix} 1 \\ 0 \\ \ldots\ldots \\ 0 \end{bmatrix}. \tag{10}$$

Hence, autoregression can be interpreted as the best m-linear one-point forward predictor for the sample, and the final prediction error E_m can be determined from

$$E_m = \left| r(0) + \sum_{k=1}^{m} a_k r^*(k) \right|^2. \tag{11}$$

In our present case of ENMR signals, the data is a stationary signal, and thus autoregression can be driven backward, consequently obtaining a forward–backward predictor. Therefore, the MEM spectrum can be interpreted as being the Fourier transform of an infinite time series, where the data sample has been extended to infinity by driving the predictor window outside the data sample. The linewidth of spectral resonance is determined by the roots of AR model, $\{a_1 \ldots a_k\}$, in the experimental data analysis. For the chosen examples of 2D-ENMR in this article, the MEM spectra generated by using computer simulations confirmed the removal of signal truncation artifacts in the high resolution ENMR spectra in the presence of gaussian noise similar to that observed in the ENMR experiments using proteins.

3. Methods

3.1. Experimental 2D-ENMR of proteins

Two-dimensional ENMR data matrices were used to test the effectiveness of the MEM method over FFT analysis in studying the truncated electrophoretic interferograms in the electrophoretic flow dimension. In the first example, we re-analyzed a previously published 2D-ENMR data matrix acquired from a solution mixture containing proteins BSA and ubiquitin [3]. In the second example, a new 2D-ENMR data set was obtained from a lysozyme/D_2O sample by using a high-resolution Varian Unity Plus 500 NMR spectrometer equipped with an actively-shielded z-gradient. In the lysozyme experiment, a CA-ENMR U-tube of 18 bundled capillaries (length $\sim$ 10 cm, ID = 250 μm, and $A = 0.884\ \mathrm{mm}^2$) was used. In the BSA and ubiquitin investigations, a U-shaped glass tube (OD = 2.5 mm, length = 10 cm, and $A = 3.758\ \mathrm{mm}^2$) was employed [3]. The inner glass surfaces of the ENMR cells were carefully cleaned to reduce the electroosmotic effect [11]. The ENMR tubes were soaked for 2–3 min each in 1 M sodium hydroxide and 1 M hydrochloride acid and washed with distilled water after each step. The glass surface of each sample tube was treated for 2 min with a 2% (γ-glycidoxypropyl)-trimethoxysilane

solution prepared with 1 part distilled deionized water, 4 parts methanol, and a few drops of concentrated acetic acid. The tubes were then rinsed with distilled deionized water. Finally, the sample tube was injected with 0.1% methyl cellulose in water and was allowed to soak for 2 min in order to coat the inner glass surface. The sample solution was carefully injected into the CA-ENMR chamber to remove any air bubbles that may have been trapped in the capillaries.

Two platinum electrodes were placed into the sample solution reservoirs at the entrance to the two U-tube arms. The sample chambers were placed in the center of the 5 mm commercial probe from the magnet top of the NMR spectrometer. The electrodes received DC electric field pulses from an electric field/magnetic gradient generator (Digital Specialties, Inc.), which gave a rising time of 1 ms/mA at a maximum output voltage of 1000 V. The pulsed-field-gradients were generated from the same device in the BSA and ubiquitin experiment. The rising time of the Varian gradient pulses employed in the lysozyme experiment was 1ms to reach the maximum gradient strength. The TTL pulses within the NMR pulse sequence program triggered the electric field pulse from spectrometer console. The amplitude and duration of electric field and gradient pulses were defined in a driver program installed in an IBM PC-486 computer in the BSA and ubiquitin experiment on the Bruker AM 500 spectrometer [3]. On the Varian NMR spectrometer, the maximum gradient strength calibrated with D_2O was 673.0 mT m^{-1} (25 °C) using the Stejskal–Tanner PFGNMR method [19,30].

The 2D-ENMR data matrix $S(E_{dc}, t_2)$ was first Fourier transformed in the chemical shift dimension and displayed using the FELIX processing package (Molecular Simulations, inc.). The resulting Felix data $S(E_{dc},f_2)$ was then read by an in-house Matlab 7.0 program. It was then further transformed using MEM into the frequency domain in the electrophoretic flow dimension using the Signal Processing toolbox (Mathworks, Inc.). Burg's version of AR model was used to generate an optimized order for MEM using Sigfusson's criteria [31]. The data matrix $S(E_{dc},f_2)$ was also Fourier transformed as a control variable.

3.2. Computer simulations

Single and two-component ENMR flow interferograms were simulated under experimental conditions to validate our MEM analysis at different Gaussian noise levels and degrees of signal truncation. A time-domain two-component synthetic electrophoretic flow signal was generated as

$$f(t) = \cos(2\pi P_1 \mu_1 I_{dc}^{\text{step}} t) + \cos(2\pi P_2 \mu_2 I_{dc}^{\text{step}} t) + D^{*}\text{Gaussian}(t) \quad (12)$$

assuming a U-shaped ENMR sample tube, 'D' as the noise level, and $P_1 = P_2 = K\Delta/2\pi\kappa A; I_{dc}^{\text{step}}$ as the increment size of electric current passing through the sample mixture solution with their individual electrophoretic mobilities μ_1 and μ_2. Monte-Carlo simulations with 1000 iterations were performed to generate ENMR spectral noise at a corresponding ENMR interferogram length by using a random number generator. Signal-to-Noise ratio (S/N) was defined as $1/D$, resulting in $S/N = 1$ to ∞ for $D = 1$ to 0. The objective was to achieve a high spectral resolution in the electrophoretic flow dimension and to analyze the precise ENMR peak positions and line widths of proteins with MEM.

4. Results and discussion

Two sets of two-dimensional STE-ENMR data were used to demonstrate the superiority of MEM over FFT method in the improvement of the ENMR signal resolution in the electrophoretic flow dimension. The first experimental data was acquired from a 5 mM lysozyme in D_2O solution, using a CA-ENMR sample chamber at pH = 5.9 ($\kappa = 2.88$ mS cm^{-1}) on the Varian Unity-500 spectrometer at 25 °C. An electric current was applied from 0.0 to 1.4 mA at 0.1 mA increments. Adjustments were made to find the optimal electric current in order to minimize the heat-induced convection at the maximum electric field. The second data set was obtained from the previously published work on the ubiquitin and BSA protein mixture at 25 °C [3]. A time domain data matrix (1024×21) was acquired by using a 21-step process in which the electric field E_{dc} was incremented from 0.0 to 38.45 V cm^{-1} on a Bruker-500 AMX spectrometer [3]. A one-dimensional Fourier transformation in the chemical shift dimension was performed in order to convert the lysozyme time-domain data into the frequency domain spectra for all FIDs (Fig. 1A). The data truncation of the electrophoretic interferogram is shown using the lysozyme resonance at 3.3 ppm (Fig. 1B). A second Fourier transformation of the lysozyme data matrix with respect to the incrementing electric field gave the 2D-ENMR spectrum of the protein resonances as pairs of mirror resonances relative to the zero axis in the flow dimension. Severe artificial line broadening in the electrophoretic flow dimension was introduced by the second FFT processing (Fig. 2A). The MEM method gave a 5.5-fold increase in spectral flow resolution in the flow dimension over the FFT analysis (Fig. 2B). The MEM measured electrophoretic mobility for lysozyme was 0.75×10^{-4} cm^2 V^{-1} s^{-1}, a value consistent with the reported value of 1.3×10^{-4} cm^2 V^{-1} s^{-1} acquired under different experimental conditions [16]. Similarly, MEM analysis of the 2D frequency domain spectrum of ubiquitin and BSA proteins improved the protein signal resolution in the flow dimension (Fig. 3A). The electrophoretic mobilities of BSA and ubiquitin from the MEM analysis were 1.9×10^{-4} and 8.7×10^{-5} cm^2 V^{-1} s^{-1}, respectively (Table 1). This gives a factor of 3.4 and 5.7 resolution enhancements for ubiquitin and BSA, respectively, as compared to the FFT analysis (Fig. 3B). In addition, the spectral line shapes were improved dramatically in the flow dimension, whereas similar resonance frequencies were obtained from both analy-

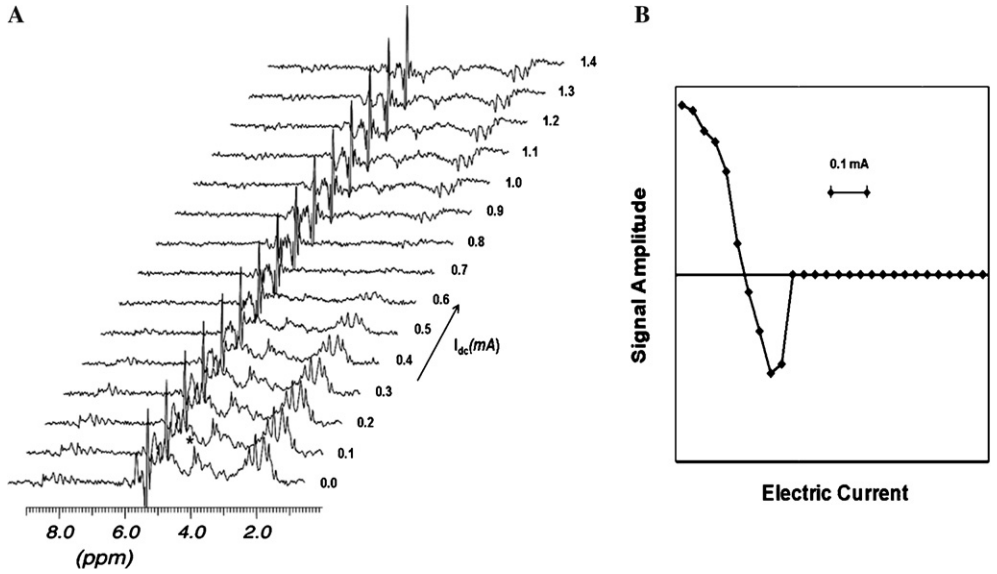

Fig. 1. (A) Two-dimensional phase-sensitive ENMR spectra of 5 mM lysozyme collected from the stimulated echo ENMR sequence on a Varian Innova 500 MHz spectrometer. A 5 mm commercial gradient probe was used to acquire 512 complex time-domain data points with 128 averages as a function of increasing electric current (0–1.4 mA) with a duration of 0.61 s. Data were zero filled to 4096 points prior to Fourier transformation. The 90° RF pulse width was 5.2 μs, the sampling interval was 62.5 μs, and relaxation delay was 3 s. The labeling and crusher gradients g and g_c were 513.5 and 513.5 mT/m with durations $\delta = 2$ ms and $\delta_c = 8$ ms, respectively. The maximum gradient strength was 673.0 mT/m, obtained from the Stejskal–Tanner diffusion calibration experiment at 25 °C. (B) Typical truncation and zero filling of electrophoretic interferogram is displayed from the lysozyme peak at 3.3 ppm.

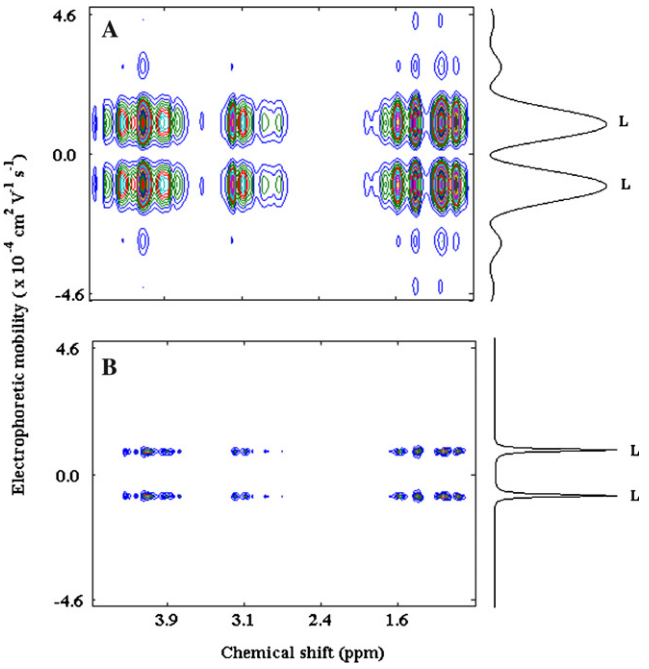

Fig. 2. 2D-ENMR spectra of lysozyme analyzed in the flow dimension using (A) FFT method for comparison and (B) MEM method employing a model order 3. In the FFT method, data in the flow dimension was zero filled to 256 time-domain data points before Fourier transformation. Spectral width in flow dimension is 19.0×10^{-4} cm^2 V^{-1} s^{-1} using MEM method. The spectral projection in the flow dimension at chemical shift 3.3 ppm is shown for comparison of FFT and MEM spectra. The MEM spectra are free of truncation artifacts with improved flow resolution.

ses. The protein spectral patterns in the chemical shift dimension were unchanged as observed in the horizontal spectral projections from both methods (Fig. 3).

Computer simulations with corresponding experimental ENMR parameters were used to generate synthetic electrophoretic flow interferograms and confirmed that MEM introduced no truncation artifacts in the flow dimension. The MEM flow resolution enhancement of a single component over FFT was calculated as a function of increasing length (L) of oscillation curve at different S/N ratios. The flow interferogram of a single component with oscillation period 'T' was analyzed at different truncation degrees and in experimental noise conditions to determine the minimum oscillation period required for a reliable MEM analysis (Fig. 4A). Incorporating different experimental noise signals restricted the minimum length of the electrophoretic interferogram for accurate measurement of electrophoretic mobility. From the single component experiment, at least $T/2$ is needed to get a reliable MEM spectrum without introducing artifacts within the experimental noise level (Fig. 4B). Artifacts or spurious peaks were observed in MEM analysis in the presence of high noise levels or high degree of data truncation (Fig. 4). Since these artifacts were also from the signal truncation and non-perfect forward–backward signal prediction, the spurious peaks occurred at the locations of a subset of FFT artifacts. The MEM flow resolution enhancement of a single- and two-component system over FFT was calculated using the length of oscillation curve similar to the experimental data under similar S/N ratios. Theoretical 6-fold MEM resolution enhancement for a single component (Fig. 5A and B) was in close agreement with the 6-fold enhancement observed in the corresponding lysozyme electrophoretic oscillation curve ($L \sim 3/4T$) with experimental noise $D = 0.3$ or $S/N = 3.3$. To validate the advantage of the MEM method

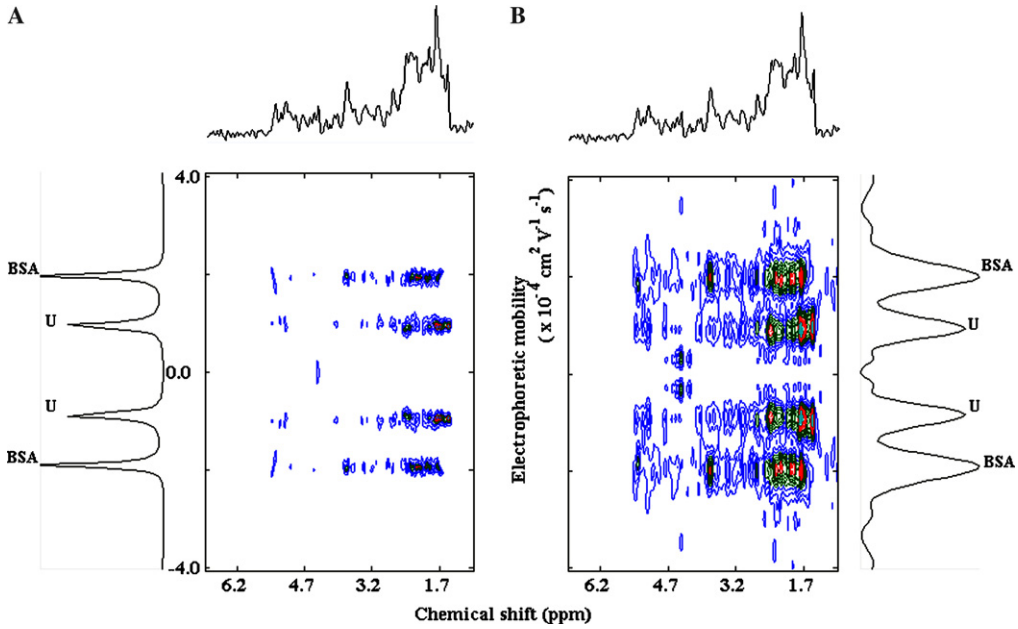

Fig. 3. Two-dimensional electrophoretic NMR spectrum of the BSA and ubiquitin (U) mixture after Fourier transformation in the chemical shift dimension followed by either (A) MEM analysis with optimized AR model order of 10 or (B) FFT after 256 time point zero filling in the electrophoretic flow dimension. The spectra in the chemical shift dimension were shown in horizontal spectral projections. The representative spectra in the flow dimension were obtained at the chemical shift resonance of 1.7 ppm.

Table 1
Comparison of ENMR flow resolution in MEM versus FFT analysis

Protein	Frequency ($\times 10^{-4}$ cm^2 V^{-1} s^{-1})		Linewidth ($\times 10^{-4}$ V^{-1} cm^{-2} s^{-1})		Resolution		Resolution enhancement	Electrophoretic mobility ($\times 10^{-4}$ cm^2 V^{-1} s^{-1})		
	MEM	FFT	MEM	FFT	MEM	FFT	MEM/FFT	MEM	FFT	Literature
BSA	1.9	2.0	0.12	0.69	15.9	2.8	5.7	1.9	2.0	1.6 [3]
Ubiquitin	0.87	0.81	0.18	0.57	4.7	1.4	3.4	0.87	0. 81	0.77 [3]
Lysozyme	0.75	0.97	0.15	0.11	5.0	0.9	5.5	0.75	0.97	1.3 [16]

over the FFT method in terms of improved resolution, we generated (Fig. 5C) and Fourier-transformed (Fig. 5D) an electrophoretic interferogram with extended length under experimental noise conditions. Calculated electrophoretic mobility was equal to the input value used for simulations, which is similar to that obtained from the MEM spectral analysis (Fig. 5B). Similarly, experimental conditions to resolve ENMR spectra of a two-component protein system of BSA and ubiquitin were simulated to determine the resolution enhancement factors of the MEM method. The component 1 was allowed to have a half oscillation period (like ubiquitin, $\mu = 1.0 \times 10^{-4}$ cm^2 V^{-1} s^{-1}) and component 2 was allowed to have a full oscillation period (like BSA, $\mu = 2.0 \times 10^{-5}$ cm^2 V^{-1} s^{-1}) (Fig. 6A). The flow resolution (Eq. (3)) enhancement factors R_{ENMR} obtained from Burg's MEM method compared with FFT for both components were calculated as a function of different noise levels (data not shown). MEM resolution enhancement of component 1 is 3.5-fold (Fig. 6B), which is close to the 3.4-fold increase from ubiquitin's experimental measurements (electrophoretic oscillation curve $\sim T/2$ with corresponding experimental noise level $D = 0.3$). Mobility changes of $\sim$10% were observed. The flow resolution of the second component was increased by 6-fold, which was in close agreement with the experimentally measured BSA resolution enhancement of 5.7 (Fig. 6B). Since the MEM method dramatically improves the flow resolution, ENMR can resolve NMR spectra of multiple protein components in solutions in their physiological conditions (high salt concentrations), by alleviating heat-induced convection effects. Hence, multidimensional ENMR is potentially applicable for simultaneous structure determination of multiple protein components.

5. Conclusions

The MEM analysis improves the spectral line shape and flow resolution in the electrophoretic flow dimension in multi-dimensional ENMR of proteins. The reliability of Burg's MEM analysis was verified using synthetic electrophoretic oscillation curves in typical ENMR experimental conditions. Further improvement in electrophoretic flow

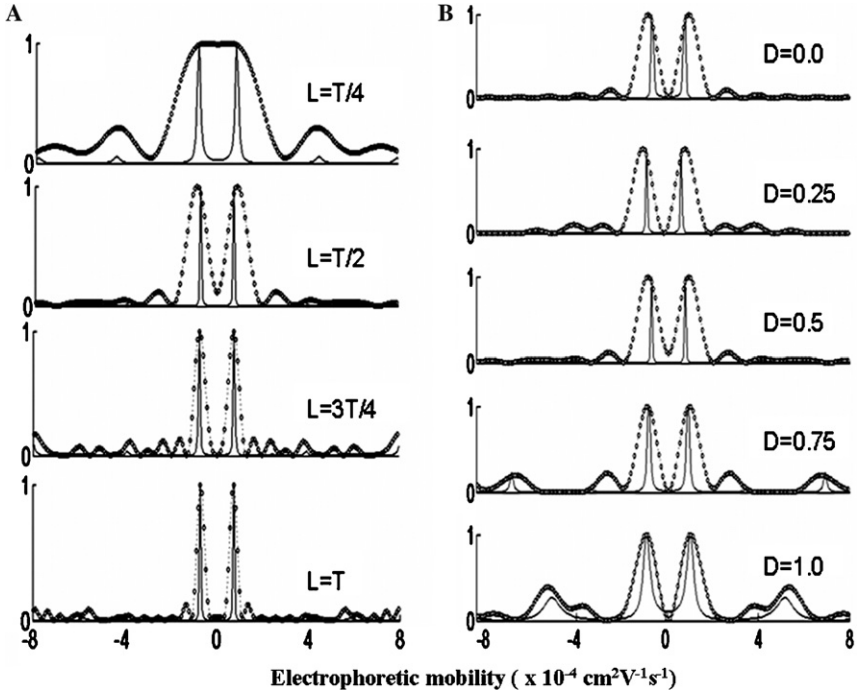

Fig. 4. Numerical simulation of single component ENMR spectra obtained at different S/N levels and varying degree of signal truncation (represented by the signal length 'L') in the cosinusoidal electrophoretic interferogram using Burg's MEM method (solid line) and FFT (—○—○—). (A) ENMR spectra as a function of increasing L from $T/4$ to T in steps of $T/4$ under noise conditions of $S/N = 2$ ($D = 0.5$). This simulation demonstrated improved flow resolution in MEM analysis. (B) The signal simulation of a half wavelength $L = T/2$ electrophoretic interferogram, with decreasing flow resolution and increasing noise level in the MEM analysis. 'T' designates the period of the cosine curve of 32 data points, generated using $\mu = 1.0 \times 10^{-4}$ cm^2 V^{-1} s^{-1} and the other ENMR parameters in the BSA and ubiquitin experiment. The FFT method introduces severe truncation artifacts.

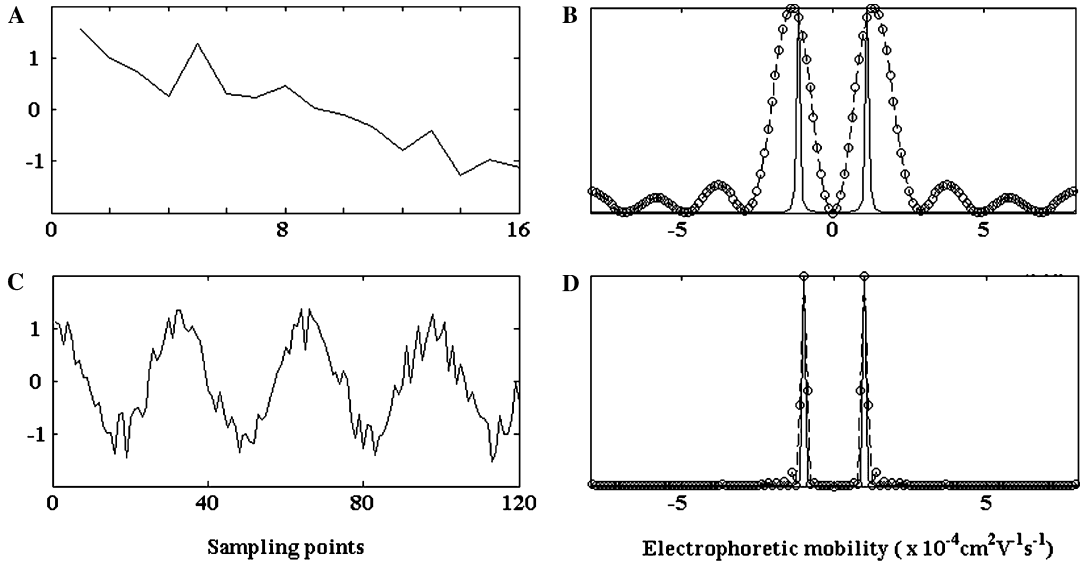

Fig. 5. (A) Simulated electrophoretic interferogram under experimental noise conditions ($S/N = 3.3$; $D = 0.3$) and $L = (3/4)T$, corresponding to the lysozyme experiments. (B) ENMR spectra of data using Burg's MEM method (solid line) and FFT (—○—○—), demonstrating improved flow resolution in MEM analysis without truncation artifacts. (C) Validation of this method using signal simulation of electrophoretic interferogram with $L > 3T$. (D) With minimum truncation artifacts, both MEM and FFT gave similar ENMR spectra. The electrophoretic mobility $\mu = 1.0 \times 10^{-4}$ cm^2 V^{-1} s^{-1} was used in the simulations.

resolution may be possible by using a high-voltage electric field driver and horizontal ENMR capillary sample cells [32]. Technical advancement in high-resolution nD-ENMR will enable us to study detailed structural changes of multiple proteins interacting in a biochemical reaction in biological signaling events [33].

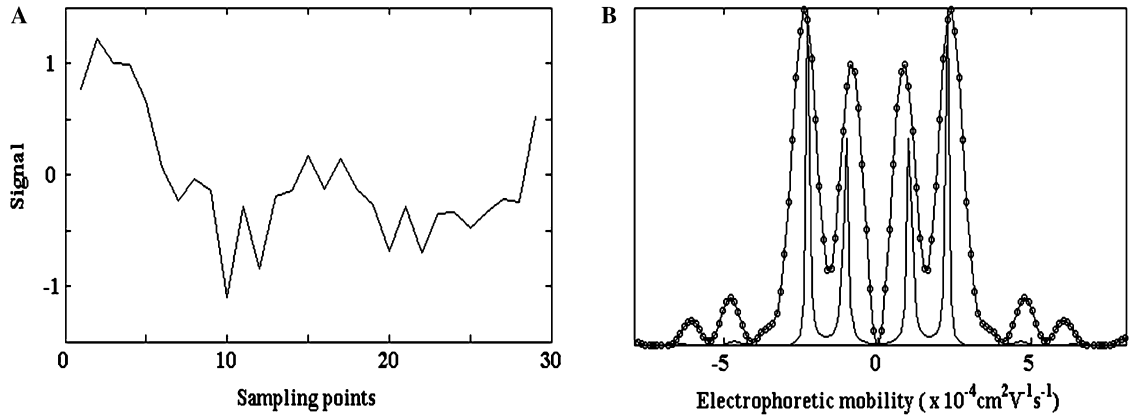

Fig. 6. Simulated electrophoretic interferogram (A) and corresponding ENMR spectra (B) of a two-component system using MEM (solid line) versus FFT (—○—○—) under experimental noise conditions and truncation levels that are similar to the BSA and ubiquitin experiment. Electrophoretic mobilities $\mu_1 = 1 \times 10^{-4}$ cm^2 V^{-1} s^{-1} and $\mu_2 = 2 \times 10^{-4}$ cm^2 V^{-1} s^{-1} were used for component 1 and component 2 in the simulations, respectively.

Acknowledgments

The work was supported in part by grants from the National Institutes of Health (NIH RR12774-01), the National Science Foundation (NSF MCB-9707550), and the American Chemical Society Petroleum Research Funds (PRF#32308-G4). We thank Dr. Dinshaw Patel at Memorial Sloan Kettering Cancer Center for providing the Varian Unity Plus 500 MHz NMR spectrometer. We also thank Dr. Kaung-Ti Yung of Magnetic Resonance Research Center, Department of Radiology, University of Pittsburgh, for editorial suggestions.

References

[1] K. Wuthrich, NMR of Proteins and Nucleic Acids, John Wiley, New York, 1986.
[2] R.R. Ernst, G. Bodenhausen, A. Wokaun, Principles of Nuclear Magnetic Resonance in One and Two Dimensions, Oxford University Press (Clarendon), London/New York, 1987.
[3] Q. He, Y. Liu, T. Nixon, High-field electrophoretic NMR of mixed proteins in solution, J. Am. Chem. Soc. 120 (1998) 1341.
[4] M. Holz, O. Lucas, C. Muller, NMR in the presence of an electric current. Simultaneous measurements of ionic mobilities, transfer numbers, and self-diffusion coefficients using an NMR pulsed-gradient experiment, J. Magn. Reson. 58 (1984) 294.
[5] M. Holz, C. Muller, NMR measurement of internal magnetic field gradients caused by the presence of an electric current in electrolyte solutions, J. Magn. Reson. 40 (1980) 595.
[6] M. Holz, C. Muller, Direct measurement of single ionic drift velocities in electrolyte solutions. An NMR method, Ber. Bunsen. Phys. Chem. 86 (1982) 141.
[7] T.R. Saarinen, C.S. Johnson Jr., High-resolution electrophoretic NMR, J. Am. Chem. Soc. 110 (1988) 3332.
[8] Q. He, C.S. Johnson, Two-dimensional electrophoretic NMR for the measurement of mobilities and diffusion in mixtures, J. Magn. Reson. 81 (1989) 435.
[9] C.S. Johnson, Q. He, Electrophoretic NMR, in: W.S. Warren (Ed.), Advances in Magnetic Resonance, Academic Press, San Diego, 1989, p. 131.
[10] Q. He, C.S. Johnson, Stimulated echo electrophoretic NMR, J. Magn. Reson. 85 (1989) 181.
[11] Q. He, Electrophoretic Nuclear Magnetic Resonance, North Carolina, Chapel Hill, Ph.D. Thesis, 1990.
[12] Q. He, D.P. Hinton, C.S. Johnson Jr., Measurement of mobility distributions for vesicles by electrophoretic NMR, J. Magn. Reson. 91 (1991) 654.
[13] K.F. Morris, C.S. Johnson Jr., Mobility-ordered two-dimensional nuclear magnetic resonance spectroscopy, J. Am. Chem. Soc. 114 (1992) 776.
[14] K.F. Morris, C.S. Johnson Jr., Mobility-ordered 2D NMR spectroscopy for the analysis of ionic mixtures, J. Magn. Reson. Ser. A 100 (1993) 67.
[15] Q. He, W. Lin, Y. Liu, E. Li, Three-dimensional electrophoretic NMR correlation spectroscopy, J. Magn. Reson. 147 (2000) 361.
[16] Q. He, Y. Liu, H. Sun, E. Li, Capillary array electrophoretic NMR of proteins in biological buffer solutions, J. Magn. Reson. 141 (1999) 355.
[17] Q. He, Z. Wei, Convection compensated electrophoretic NMR, J. Magn. Reson. 150 (2001) 126.
[18] J.P. Burg, A New Analysis Technique for Time series Data. Enschede: Advanced Study Institute on Signal Processing, Enschede: NATO, 1968.
[19] J.E. Tanner, Use of the stimulated echo in NMR diffusion studies, J. Chem. Phys. 52 (1970) 2523.
[20] S.M. Kay, S.L. Marple, Modern Spectral Estimation—Theory and Application, Prentice-Hall, Englewood Cliffs, NJ, 1981.
[21] W. Press, S. Teukolsky, W. Vetterling, Numerical Recipes in C: The Art of Scientific Computing, Cambridge University Press, Cambridge,UK, 1992.
[22] P. Stoica, R.L. Moses, Introduction to Spectral Analysis, Prentice-Hall, Englewood Cliffs, NJ, 1997.
[23] S.L. Marple, Digital Spectral Analysis, Prentice-Hall, Englewood Cliffs, NJ, 1987.
[24] E.D. Laue, J. Skilling, J. Staunton, S. Sibisi, R. Brereton, Maximum entropy method in NMR spectroscopy, J. Magn. Reson. 62 (1985) 437.
[25] P.J. Hore, NMR data processing using the maximum entropy method, J. Magn. Reson. 62 (1985) 561.
[26] M. Stephenson, Linear prediction and maximum entropy methods in NMR spectroscopy, Prog. NMR Spectrosc. 20 (1988) 515.
[27] G. Brinkmann, U.H. Melchert, W. Drher, J. Brossmann, H. Tressing, C. Muhle, M. Reuter, M. Heller, Application of the maximum entropy method for evaluating phosphorus-31-magnetic resonance spectra in patients with liver metastasis, Invest. Radiol. 30 (1995) 150.

[28] A.S. Stern, J.C. Hoch, Maximum Entropy Reconstruction in NMR, in: D.M. Grant, R.K. Harris (Eds.), Encyclopedia of NMR, John Wiley, Chichester, 1996.
[29] M. Ostafin, D. Lemanski, B. Nogaj, Comparison of some resolution enhancement methods applied to Cl-35-NQR nutation spectroscopy, Appl. Magn. Reson. 18 (2000) 137.
[30] E.O. Stejskal, J.E. Tanner, Spin diffusion measurements:spin echos in the presence of a time-dependent field gradient, J. Chem. Phys. 42 (1965) 288.
[31] T.I. Sigfusson, K.P. Emilsson, P. Mattocks, Application of the maximum-entropy technique to the analysis of de Haas-van Alphen data, Phys. Rev. B 46 (1992) 10446.
[32] E. Li, Q. He, Constant-time multidimensional electrophoretic NMR, J. Magn. Reson. 156 (2002) 181.
[33] Q. He, X. Song, Electrophoretic Nuclear Magnetic Resonance in Proteomics: Toward High-Throughput Structural Characterization of Biological Signaling Processes, in: G.B. Smejkal, A. Lazarev (Eds.), Separation Methods in Proteomics, Marcel Dekker, Inc., New York, 2005, p. 489.